

## Improvement of opipramol base solubility by complexation with $\beta$ -cyclodextrin

K. Majewska<sup>a</sup>, A. Skwierawska<sup>a</sup>, B. Kamińska<sup>a</sup> and M. Przeźniak-Welenc<sup>b</sup>

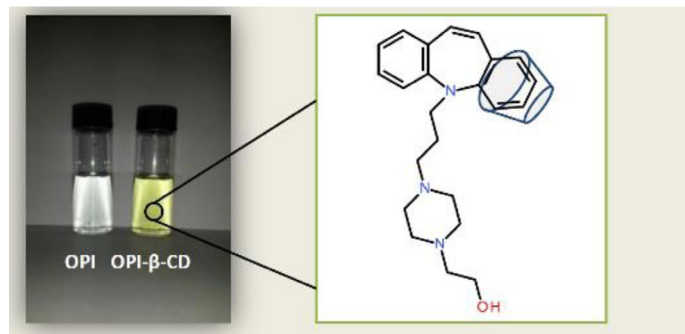
<sup>a</sup>Department of Chemistry and Technology of Functional Materials, Gdańsk University of Technology, Gdańsk, Poland; <sup>b</sup>Department of Solid State Physics, Gdańsk University of Technology, Gdańsk, Poland

### ABSTRACT

Opipramol (OPI), a tricyclic antidepressant and anxiolytic compound, is administered orally in the form of a dihydrochloride. Salt form of the drug has a higher solubility in water and hence bioavailability and stability. A similar effect can be achieved by closing the hydrophobic part of the drug molecule in the cyclodextrin cavity. The paper presents opipramol inclusion complexes with beta-cyclodextrin ( $\beta$ -CD) in 1:1 molar ratio. Studies on the formation of inclusion complexes were carried out both in solution and in the solid state. The formation and physicochemical characterisation of the complexes were determined by UV spectroscopic measurement (UV-vis), Fourier Transform Infrared (FTIR) Spectroscopy, <sup>1</sup>H Nuclear Magnetic Resonance (<sup>1</sup>H NMR, 2D NOESY NMR), thermoanalytical methods (TGA – Termogravimetric analysis, DSC – differential scanning calorimetry), X-ray diffractometry (XRD) and scanning electron microscopy (SEM). The phase solubility profile with  $\beta$ -CD was classified as the A<sub>N</sub>- type, indicating the formation of the inclusion complex with a drug.

### KEYWORDS

Opipramol base;  $\beta$ -cyclodextrin; inclusion complex; co-grinding method; freeze-drying method



### Introduction

The typical feature of many drugs administered orally and in the form of infusions is their limited water solubility. Pharmaceutical companies solve this problem by choosing the right crystallographic forms and micronisation. In case of insufficient effect, the active substances are converted into salts or complexes (1, 2).

Undoubtedly, salt formation has been the most popular strategy for several decades to enhance their solubility, dissolution rate as well as stability. In numerous technologies, hydrochlorides are obtained by reaction with concentrated hydrochloric acid or gaseous HCl, as in the case of Opipramol (OPI) (Figure 1) which is against the

principles of green technologies. This is why alternative forms of drugs characterised by high bioavailability are prospected. One of the noteworthy solutions is the use of cyclodextrins as complexing agents of drugs.

Cyclodextrins are cyclic ( $\alpha$ -1,4)-linked oligosaccharides of  $\alpha$ -D-glucopyranose obtained by enzymatic degradation of starch. CDs are cone-like structures open at both rims. Due to their hydrophilic outer surface, which facilitates solubility in water, and a hydrophobic cavity, the CDs are described as a 'micro heterogeneous environment' (3) and the latter as container molecules. CDs are capable of forming complexes by hydrophobic interaction of lipophilic cavity with lipophilic guest molecule(s)

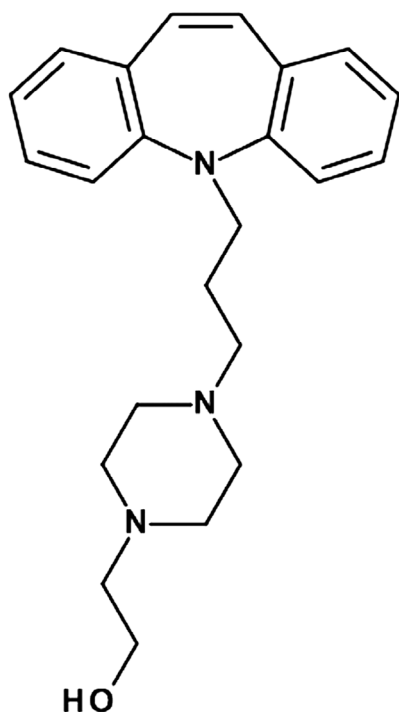


Figure 1. Molecular structure of OPI.

of an appropriate size or sizes. Therefore, the CDs are host molecules for a wide variety of organic and inorganic molecules or ions.

Cyclodextrin complexes with drug molecules are formed by non-covalent interactions between the incorporated molecule and cavity of the host. During the 'guest-host' complex synthesis, covalent bonds are not formed and not broken. The complex formation is the process of dynamic equilibrium wherein the included molecule is alternately connected and dissociated from the cavity of cyclodextrin (4). Complexing properties of various cyclodextrins depend on the cavity size, molecular shape of the guest molecule and the hydrophobic cyclodextrin cavity (5).

In this study, an innovative solid binary system of OPI with  $\beta$ -CD was prepared using co-grinding (CG) and freeze-drying (FD) techniques. The mechanism of interactions between OPI and  $\beta$ -CD was studied using the phase solubility method. Moreover, the solid OPI- $\beta$ -CD complexes were characterised by UV spectroscopic measurements (UV-vis), Fourier Transform Infrared (FTIR) Spectroscopy,  $^1\text{H}$  Nuclear Magnetic Resonance ( $^1\text{H}$  NMR, 2D NOESY NMR), thermoanalytical methods (TGA – Thermogravimetric analysis, DSC – Differential Scanning Calorimetry), X-ray diffractometry (XRD) and Scanning Electron Microscopy (SEM). The dissolution properties were examined according to the rotating basket method in distilled water.

## Experimental

### Materials

Opi Pramol and  $\beta$ -cyclodextrin were purchased from Sigma Aldrich. Deionised water (HLP SPRING,  $T = 20.7^\circ\text{C}$ ,  $\kappa = 2.70\ \mu\text{S}$ ) was used throughout the study.

### Phase solubility studies

Phase solubility studies were carried out according to the method reported by Higuchi and Connors (6). OPI (73 mg) was added to aqueous solutions of  $\beta$ -CD (concentration 0–20 mM, volume 20 mL) in a 50 mL stoppered Erlenmeyer flask. The obtained suspensions were shaken at room temperature ( $25 \pm 0.5^\circ\text{C}$ ) for 7 days. After reaching equilibrium, aliquots were withdrawn, filtered through a  $0.45\ \mu\text{m}$  membrane filter (Pureland, Poland), suitably diluted and analysed spectrophotometrically (HACH LANGE DR 6000) for opi pramol content at 253 nm. UV absorption spectra were recorded in the wavelength range from 200 to 400 nm. Each experiment was performed in triplicate.

The apparent stability constant ( $K_{1:1}$ ) molar ratio between OPI and CD were calculated from the phase solubility diagram according to the formula:

$$S_0 K_{1:1} = \text{slope} / 1 - \text{slope} \quad (1)$$

where,  $S_0$  represents the solubility of OPI in the absence of cyclodextrin.

### UV spectroscopic studies

Complex formation between OPI and  $\beta$ -CD was analysed by comparing the absorption spectra of five samples: pure OPI,  $\beta$ -CD, physical mixture (PM) of both, and freeze-dried and co-ground complex. The formal concentration of OPI and  $\beta$ -CD in each sample was 0.1 mM. The prepared solutions were stirred for 1 h, and filtered through a  $0.45\ \mu\text{m}$  membrane filter. The UV absorption spectra were recorded in the wavelength range from 200 to 400 nm against the blank distilled water using HACH LANGE UV-vis DR 6000 spectrophotometer.

### Preparation of OPI- $\beta$ -CD solid binary systems

Two distinct methods: FD and CG were used for preparation of solid binary systems consisting of OPI and  $\beta$ -CD at a 1:1 molar ratio. PM and inclusion complexes between OPI and  $\beta$ -CD were also prepared for comparison.

### Physical mixture

PM were prepared by mixing the two components in an agate mortar for 2 min.



### **Freeze-drying method**

$\beta$ -CD (113.5 mg) was dissolved in distilled water. Then, OPI was added to this solution whilst stirring, according to the appropriate ratio. The mixing of the solution was continued for 7 days. Furthermore, the aliquots were filtered through a 0.45  $\mu$ m membrane filter. The clear solution was frozen at  $-20$   $^{\circ}$ C, and then lyophilised in a freeze-dryer (Novalyph-NL 500; Savant Instruments Corp., U.S.A.) at  $-50$   $^{\circ}$ C for 24 h. The resulting powder was then sieved and homogenised by grinding in the agate mortar.

### **Co-grinding method**

CG mixture was prepared by milling OPI and cyclodextrin in a laboratory planetary ball mill with two working stations (Pulverisette 7 classic line; Fritsch GmbH, Poland) for 10 min, using the following conditions: grinding bowl size: 12 mL, rotational speed of main disc: 400 rpm. The solid residues were stored over anhydrous calcium chloride in a desiccator.

### **Physicochemical characterisation of OPI- $\beta$ -CD solid binary systems**

DSC and TGA measurements,  $^1$ H NMR, FTIR, XRD spectra were recorded for pure OPI and CDs as well for their binary systems prepared by different previously mentioned techniques.

### **Thermal analysis**

Differential scanning calorimetry (DSC) and thermal gravimetric (TGA) analyses were carried out using NETZSCH STA 449 F1-simultaneous TGA-DSC measurements. The thermal behaviour was studied by heating the samples (1–5 mg) in a covered aluminium pan and heated at a constant rate of 10  $^{\circ}$ C/min within the temperature range of 40–450  $^{\circ}$ C, and under a nitrogen flow of 40 cm<sup>3</sup>/min. The device runs under the Proteus Software.

### **Fourier-transform infrared spectroscopy**

The experimental infrared spectrum in the range of 4000–400 cm<sup>-1</sup> was recorded using a Fourier transform spectrometer Nicolet iS50 FT-IR equipped with a standard DLATGS detector and Polaris High Stability, Long Lifetime Mid-IR source. Spectra of the solid state samples were taken at room temperature.

### **Nuclear magnetic resonance studies**

The  $^1$ H NMR spectra were recorded on Varian instrument at 500 MHz.

### **Scanning electron microscopy**

The surface morphology of pure materials (OPI,  $\beta$ -CD) and binary systems was examined by means of a scanning electron microscope (EVO-40, Zeiss, Germany).

### **X-ray diffractometry**

Powder X-ray diffraction measurements were performed with the Phillips X'Pert Pro MPD diffractometer with Cu K $\alpha$  radiation within the  $2\theta$  range of 5–60  $^{\circ}$ C.

### **Dissolution studies**

The dissolution of pure opipramol base, opipramol dihydrochloride and the prepared binary systems was performed using ERWEKA dissolution tester. The dissolution medium consisted of 900 mL of distilled water. A sample in the form of powder, equivalent to 6 mg opipramol base of the formed systems was spread on the surface of the dissolution medium. The temperature was maintained at  $37 \pm 0.5$   $^{\circ}$ C and the stirring speed was 50 rpm. The total dissolution time was 120 min. At the selected time intervals, the system automatically withdrew 1 mL aliquots from the dissolution medium, filtered them and simultaneously concentrations of opipramol were determined spectrophotometrically at 253 nm. Then, after the measurement, the sample was again returned to the dissolution medium. Each experiment was carried out in triplicate.

According to the method proposed by Khan (7), the dissolution profiles were evaluated on the basis of the dissolution efficiency parameter at 60 min ( $DE_{60}$ , %), calculated from the area under the dissolution curve. The  $DE_{60}$  values of the binary systems were performed using one-way analysis of variance (ANOVA) with Tukey test for single-step multiple comparison.

## **Results and discussion**

### **Phase solubility studies**

Phase solubility studies provide information on the amount of cyclodextrin to be used to determine the maximum solubility of the drug. It is generally accepted that, depending on the obtained shape of the solubility curve, several types of behaviour can be identified (8). In this study, the OPI solubility in water was checked in a wide range of concentrations of  $\beta$ -cyclodextrins. The phase solubility diagram of OPI in a  $\beta$ -CD solution is shown in Figure 2(a). The OPI solubility increases linearly with increasing cyclodextrin concentrations in the range of 2–10 mM. The coefficient of determination ( $R^2$ ) was 0.9940. An increase in the  $\beta$ -CD concentration above 10 mM does not result in a further improvement of OPI solubility. At high concentrations of  $\beta$ -CD, the self-association of poorly soluble drug and drug/cyclodextrin complexes can be found, thus the formation of the inclusion complex is less effective (9). For the OPI- $\beta$ -CD system, the solubility curve is classified as  $A_N$ -subtype of phase-solubility profiles. Similar solubility profiles for antifungal drug and (2-hydroxypropyl)- $\beta$ -CD (HP- $\beta$ -CD) were achieved by Buchanan et al. (10). The apparent

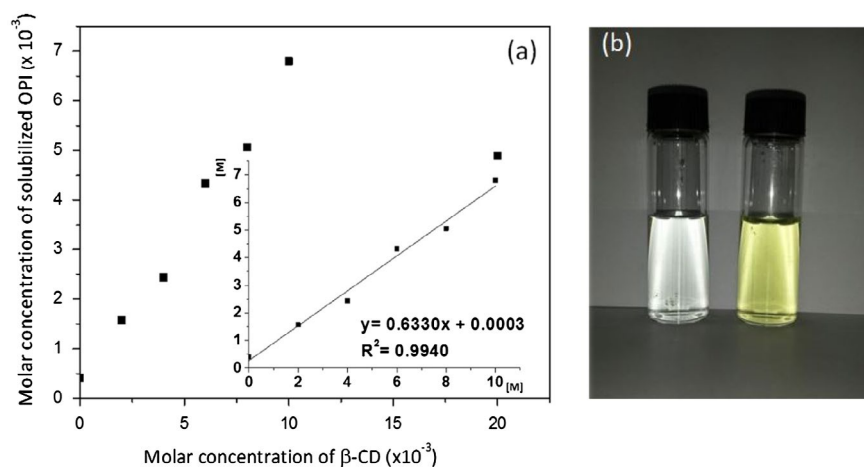


**Figure 2.** (colour online) (a) Phase solubility diagram of OPI with different  $\beta$ -CDs concentrations in distilled water at  $25 \pm 0.5$  °C; (b) colour change of the aqueous solutions of the drug by increasing the drug solubility.

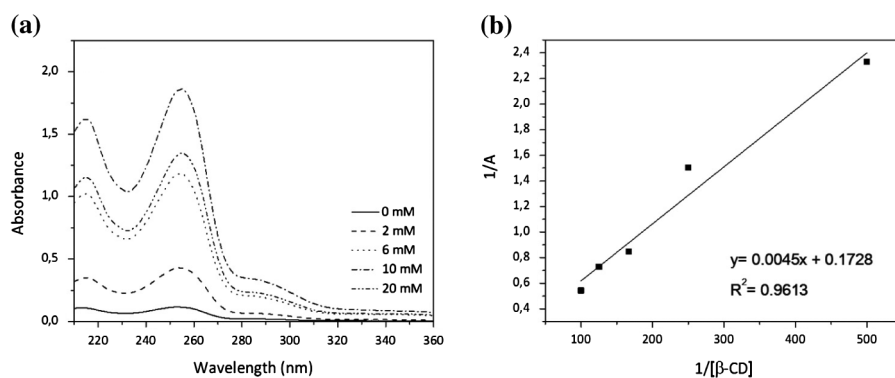


**Figure 3.** (a) Differential ultraviolet absorbance spectra of OPI in the presence of  $\beta$ -CD; and (b) reciprocal plot for  $1/A$  against  $1/[\beta\text{-CD}]$  of the OPI- $\beta$ -CD inclusion complex.

solubility constant  $K_{1:1}$  was calculated from the slope of the linear phase-solubility plot according to Equation (1) and was found to be  $4148 \text{ M}^{-1}$ . The result is within a range of  $200\text{--}5000 \text{ M}^{-1}$ . The value confirms the formation of an inclusion complex (11). The reagents molar ratio 1:1 used during preparation of the binary system was suitable to increase the drug solubility in water. Similar results were observed by Akbari et al. (12) during the preparation of inclusion complex of rosuvastatin calcium with HP- $\beta$ -CD. Due to the natural yellow taint of OPI, the increase in OPI solubility in the presence of  $\beta$ -CD in distilled water is visible to the naked eye (Figure 2(b)).

The OPI absorption spectra in aqueous solutions in the presence of different CDs concentration are shown in Figure 3(a). The increase in  $\beta$ -CD concentrations from 2 to 10 mM caused hyperchromic shifts without any shifts of  $\lambda_{\text{max}}$ . The observed hypochromic shift of the absorption spectra at the  $\beta$ -CD concentration of 20 mM may indicate the perturbation of the chromophore electrons of the drug located in the CD cavity, confirming formation

of an OPI- $\beta$ -CD complex (9). The OPI formed complex at a molar ratio of 1:1. This statement can be confirmed if a linear relationship between  $1/A$  and  $1/[\beta\text{-CD}]$  base on the Hildebrand–Benesi Equation (2) is achieved (13).

$$1/A = 1/\epsilon[G]_0K[\text{CD}] + 1/\epsilon[G]_0 \quad (2)$$

where,  $A$  is the absorbance of the OPI solution at each  $\beta$ -CD concentration (from 2 to 10 mM);  $[G]_0$  the initial concentration of OPI;  $K$  the apparent formation constant;  $[\text{CD}]$  the concentration of  $\beta$ -CD and  $\epsilon$  is the molar absorptivity. The results are presented in Figure 3(b). A good linear relationship for the  $1/A$  vs.  $1/[\beta\text{-CD}]$  with correlation coefficient of 0.9613 was noticed.

### UV spectroscopic studies

To confirm the formation of OPI- $\beta$ -CD inclusion complexes, the absorption spectra were recorded. The absorption data for OPI, pure  $\beta$ -CD, their PM and inclusion complexes are presented in Figure 4. Due to the lack of  $\beta$ -CD absorption



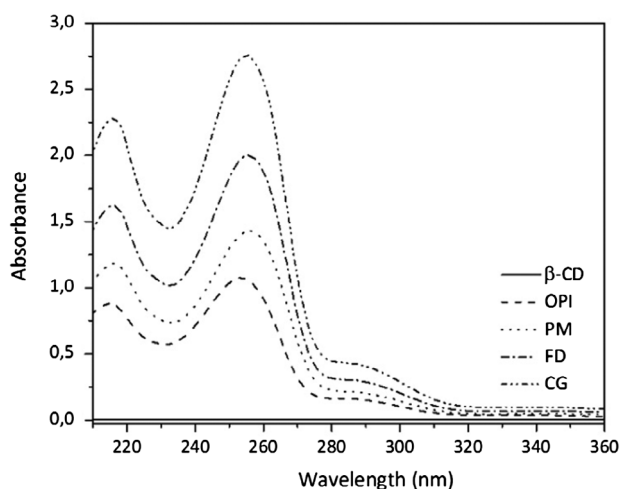


Figure 4. UV-vis absorbance spectra of the  $\beta$ -CD, OPI, PM, CG and FD inclusion complex.

throughout the whole wavelength, its absorbance can be omitted (14). In the case of a PM, a slight absorbance increase compared to the absorbance of pure drug was observed. Much better drug solubilisation for CG and FD products was noticed.

### Thermal analysis

Thermogravimetric analysis has been frequently used to show the difference between an inclusion complex and a PM of its components (15). Thermal behaviour of OPI,  $\beta$ -CD, their binary systems obtained by different ways studied by DSC and TGA are shown in Figure 5. The DSC thermogram of OPI presents a sharp endothermic pick at 100 °C consistent with its melting point. The DSC profile of  $\beta$ -CD revealed a shallow endothermic peak at 50–110 °C associated with crystal water losses, melting at 325 °C accompanied by decomposition (16). The DSC thermogram of

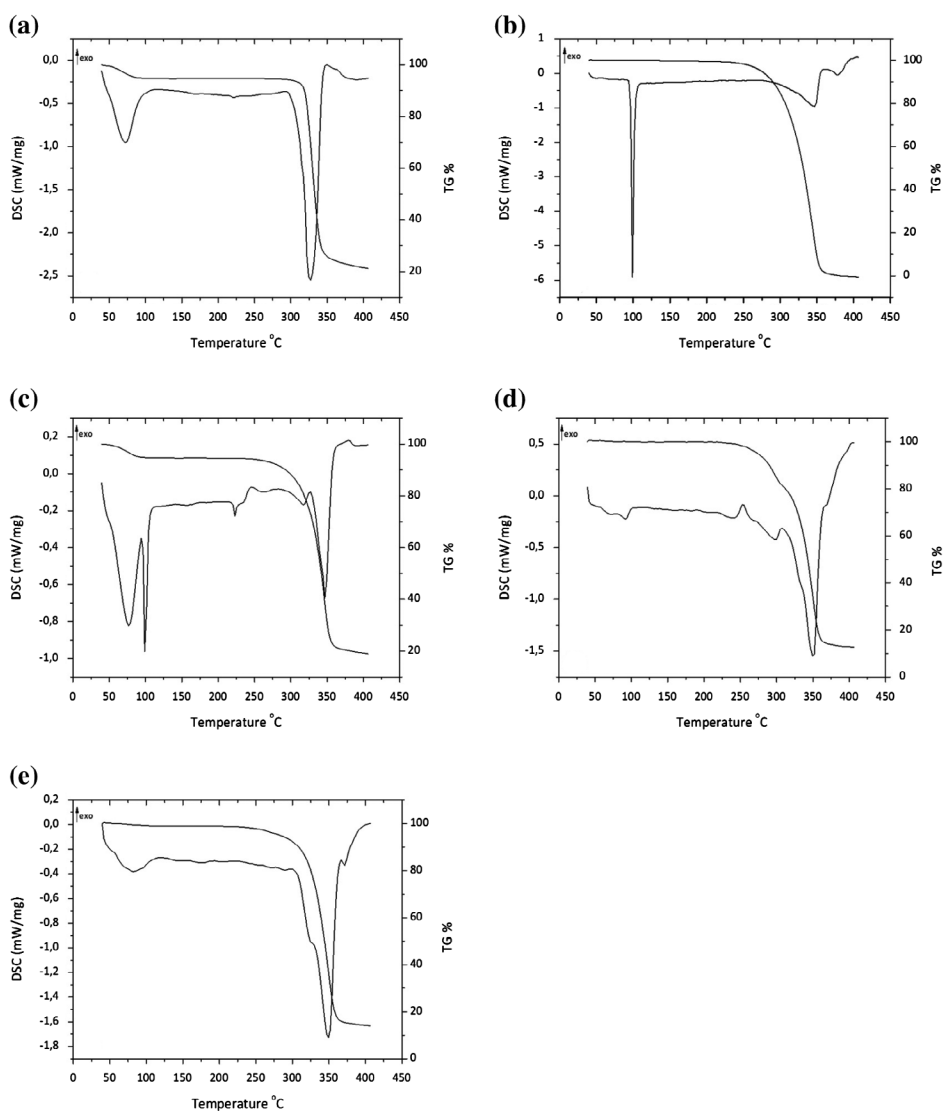


Figure 5. TGA and DSC curves of (a)  $\beta$ -CD, (b) OPI, (c) PM, (d) CG and (e) FD inclusion complex.



the PM is found to be the sum of components. The DSC profile of the complex formed by the CG method shows a very small melting endothermic effect at 100 °C, which indicates the presence of a small amount of crystalline OPI not included in the cyclodextrin cavity. The absence of the drug melting endothermic peak in the DSC thermogram for the FD system confirms the formation of an OPI- $\beta$ -CD inclusion complex (17). The broad endothermic spanning in the range of 50–110 °C corresponds to loss of strongly bound water from the cyclodextrin hydration shell (9).

The thermal behaviour of all samples, previously characterised by DSC was also investigated by TGA. In the OPI thermogram weight loss between 240 and 355 °C was observed. The pure  $\beta$ -CD exhibited weight loss at two separate temperatures. The first is in the range of 40–105 °C that corresponds to removal of water present in the cavity of the host. The second stage at 343 °C leads to the decomposition of  $\beta$ -CD. For PM of the corresponding weight loss by 4.93% between 40 and 105 °C ascribed to the water removal from  $\beta$ -CD hydrates was observed. This phenomenon was absent in both CG and FD products. Similar results were obtained by P. Mura et al. (18) in naproxen-arginine-HP- $\beta$ -CD ternary system. OPI- $\beta$ -CD binary systems prepared by CG and FD methods were characterised by higher stability as compared to the pure drug. At 363 °C, 99, 83 and 84% a significant weight loss for OPI, CG and FD inclusion complexes was noted, respectively.

#### Fourier-transform infrared spectroscopy

FTIR is a very useful method to confirm the formation of inclusion complexes (19, 20). Figure 6 illustrates FTIR spectra of pure components and their binary system prepared by different techniques.

In the IR spectrum of  $\beta$ -CD, the wide band with the absorption maximum at 3312  $\text{cm}^{-1}$  is attributed to the free O-H stretching vibration. The valence vibrations of the C-H bonds in the -CH and -CH<sub>2</sub> groups are seen at 2924  $\text{cm}^{-1}$ . The frequency observed at 1644  $\text{cm}^{-1}$  corresponds to the hydrogen bonds within cyclodextrin molecules. The absorption peaks observed in the region 1400–1200  $\text{cm}^{-1}$  could be attributed to the deformation vibrations of the C-H bonds in the primary and secondary hydroxyl groups (1412, 1366, 1335 and 1297  $\text{cm}^{-1}$ ), whilst in the range 1200–1020  $\text{cm}^{-1}$  the absorption bands correspond to valence vibrations of the C-O bonds in the ether and hydroxyl groups (1151, 1076 and 1019  $\text{cm}^{-1}$ ). The deformation vibration of C-H bonds and pulsation vibrations in glucopyranose ring appeared within 950–700  $\text{cm}^{-1}$  (19).

The FTIR spectrum of OPI shows an absorption band at 3210  $\text{cm}^{-1}$  corresponding to the O-H stretching vibration.

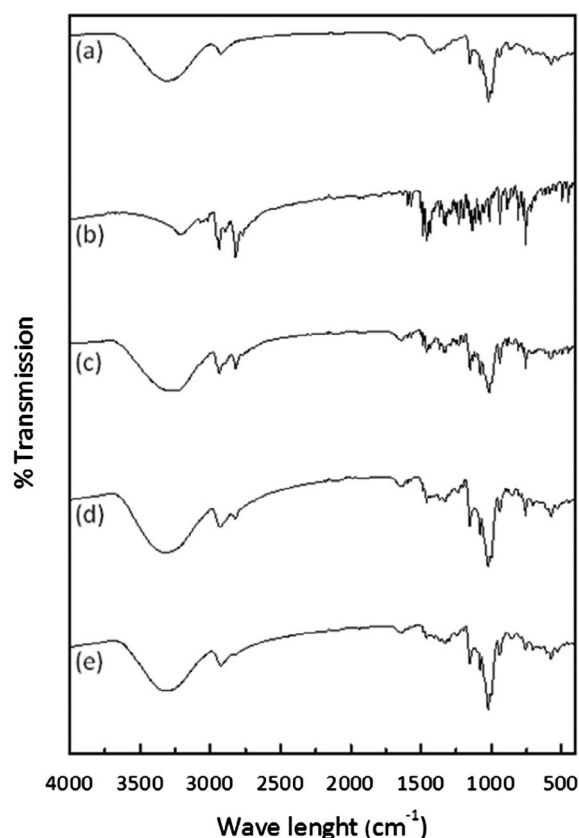
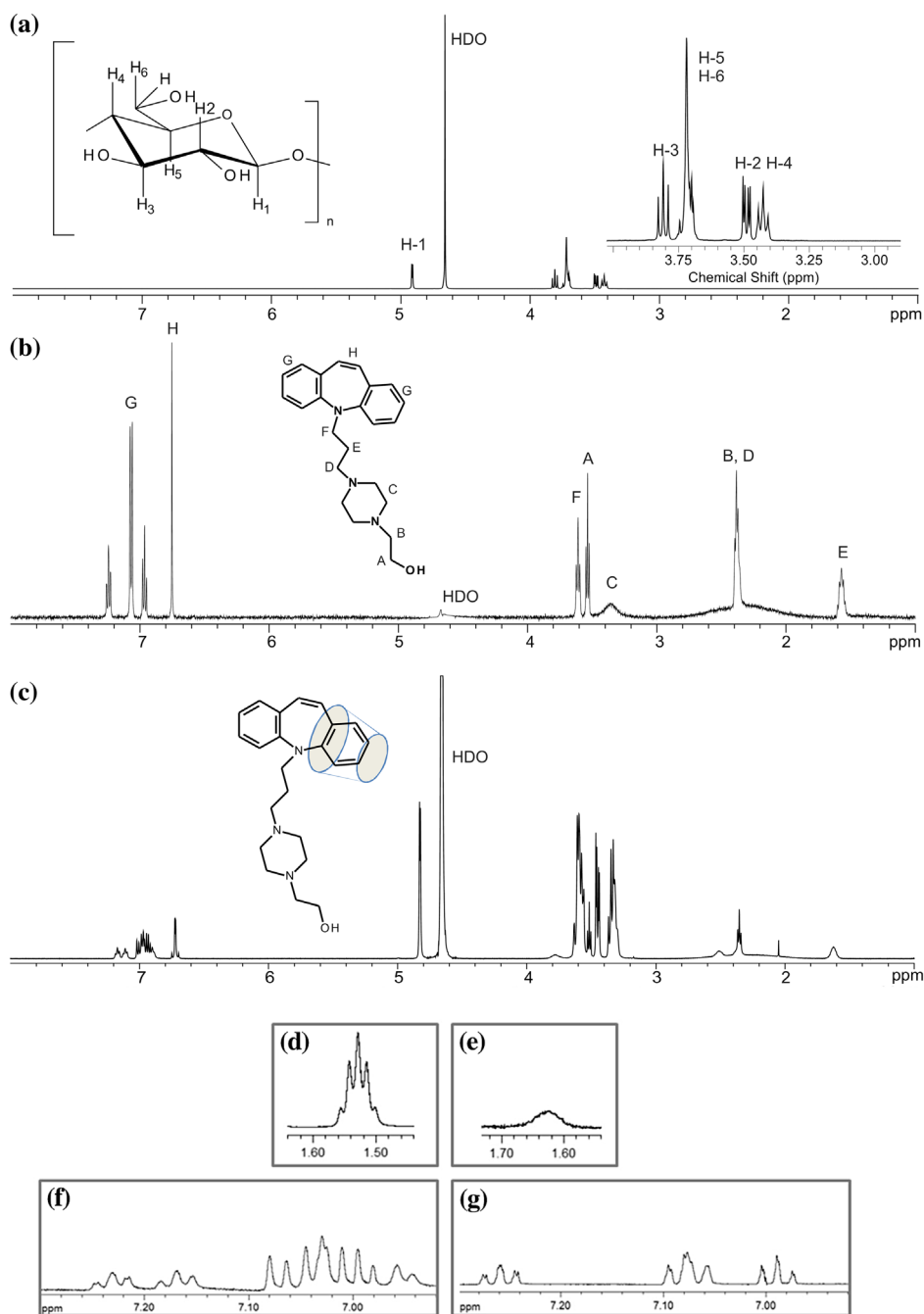


Figure 6. The Fourier transform-infrared (FTIR) spectra of (a)  $\beta$ -CD, (b) OPI, (c) PM, (d) CG and (e) FD inclusion complex.

Sharp peaks appeared in the region 3100–3000  $\text{cm}^{-1}$  (3069 and 3058  $\text{cm}^{-1}$ ) assigned to stretching aromatic bonds C<sub>Ar</sub>-H. The in-plane C<sub>Ar</sub>-H deformation bands of the phenyl ring are assigned at 1013  $\text{cm}^{-1}$  and the out-of-plane C-H deformation bands are observed at 938 and 808 and 773  $\text{cm}^{-1}$ . The strong band noted at 755  $\text{cm}^{-1}$  is due to the  $\gamma$ -C<sub>Ar</sub>-H. The C-C ring stretching is expected in the range 1260–1615  $\text{cm}^{-1}$  for phenyl rings (21, 22). In this study, the ring stretching at 1435 and 1593  $\text{cm}^{-1}$  is observed. The C-C and C-H stretching bonds in the azepine ring are registered at 1628 and 3018  $\text{cm}^{-1}$ , respectively. For OPI, the C-N stretching modes are noted in the region 1134–1230  $\text{cm}^{-1}$ . The piperazine ring stretching modes are observed at 1149, 1134, 1077, 1013, 938 and 756  $\text{cm}^{-1}$ . The vibrations of the CH<sub>2</sub> group, the asymmetric stretch  $V_{as}$ -CH<sub>2</sub>, symmetric stretch  $V_s$ -CH<sub>2</sub>, appear in the region 2936–2951 and 2810–2821  $\text{cm}^{-1}$ , subsequently (23). The region 3000–2840  $\text{cm}^{-1}$  (2935, 2908  $\text{cm}^{-1}$ ) correspond to C-H aliphatic stretching.

When the inclusion complex OPI- $\beta$ -CD is formed, a significant change in FTIR spectra between the binary system and its constituent molecule can be observed. In this study, the absorption bands in the region of 3100–3000  $\text{cm}^{-1}$  corresponding to the OPI aromatic cannot be seen in both



**Figure 7.** (colour online) <sup>1</sup>H NMR spectra of (a) β-CD, (b) OPI, (c, d, e, f, g) OPI-β-CD inclusion complex.

CG and FD complexes. The literature explains this phenomenon as the insertion of the benzene ring into the electron rich cavity of β-CD and increasing the density of the electron cloud (24). A considerable simplification of the absorption bands in the regions of 2810–2951 cm<sup>-1</sup>, 1435–1593 cm<sup>-1</sup> and 1149–756 cm<sup>-1</sup> are also observed. It can be a result of changing in the microenvironment of the guest-host system due to the formation of hydrogen bonding between the guests' heteroatom and the β-CDs' primary

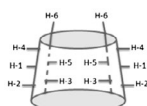
hydroxyl group located in the cavity (25). Moreover, the spectrum of the CG and FD complexes is similar to the spectra of raw β-CD. This might be indicative forming of an OPI-β-CD complex by the CG and FD methods. On the other hand, the FTIR spectra of PM illustrated the characteristic peaks of β-CD and OPI, which can be regarded as a simple superimposition of the host and guest molecules. It can be concluded as there were no interactions between the drug and the cyclodextrin in the PM (26).



## Nuclear magnetic resonance studies

To confirm the formation of the inclusion complex of OPI- $\beta$ -CD,  $^1\text{H}$  NMR method is widely used (27, 28). In general, the changes in chemical shifts displacement in both the host and guest molecules are observed. The  $^1\text{H}$  NMR spectra of pure OPI, the  $\beta$ -CD, and the inclusion complex are presented in Figure 7.

**Table 1.**  $^1\text{H}$  NMR shifts ( $\delta$ , ppm) of  $\beta$ -CD protons in the presence and absence of OPI in  $\text{D}_2\text{O}$ .

$\beta$ -CD protons		$\delta$ (free)	$\delta$ (complex)	$\Delta\delta$ ppm
H-1		4.911	4.826	-0.085
H-2		3.490	3.451	-0.039
H-3		3.808	-	overlapped
H-4		3.426	3.347	-0.079
H-5		3.719	3.595	-0.124
H-6		3.699	3.576	-0.123

The insertion of OPI into the  $\beta$ -CD caused slight shift variations in the H-3 and H-5 protons. They can be caused by non-covalent interactions between host and guest molecules. The chemical shift values of selected  $\beta$ -CD protons in the presence and absence of OPI were calculated according Equation (3) and listed in Table 1. H-5 protons are shifted with  $\Delta\delta = 0.124$  ppm. The chemical shifts of H-3 protons could not be determined, due to their overlapping. Since H-3 and H-5 face the cavity of  $\beta$ -cyclodextrin, their chemical shift changes are most likely due to the presence of one of the aromatic rings of OPI in the macrocyclic cavity. We supposed that the H-3 proton of  $\beta$ -CD displayed a larger chemical shift than H-5. It indicates that the OPI molecule can be inserted into the cavity of  $\beta$ -CD from the larger openings of the toroid.

$$\Delta\delta = \delta(\text{complex}) - \delta(\text{free}) \quad (3)$$

Chemical shifts displacements of outer protons (H-1, H-2 and H-4) are also observed. We can speculate that drug

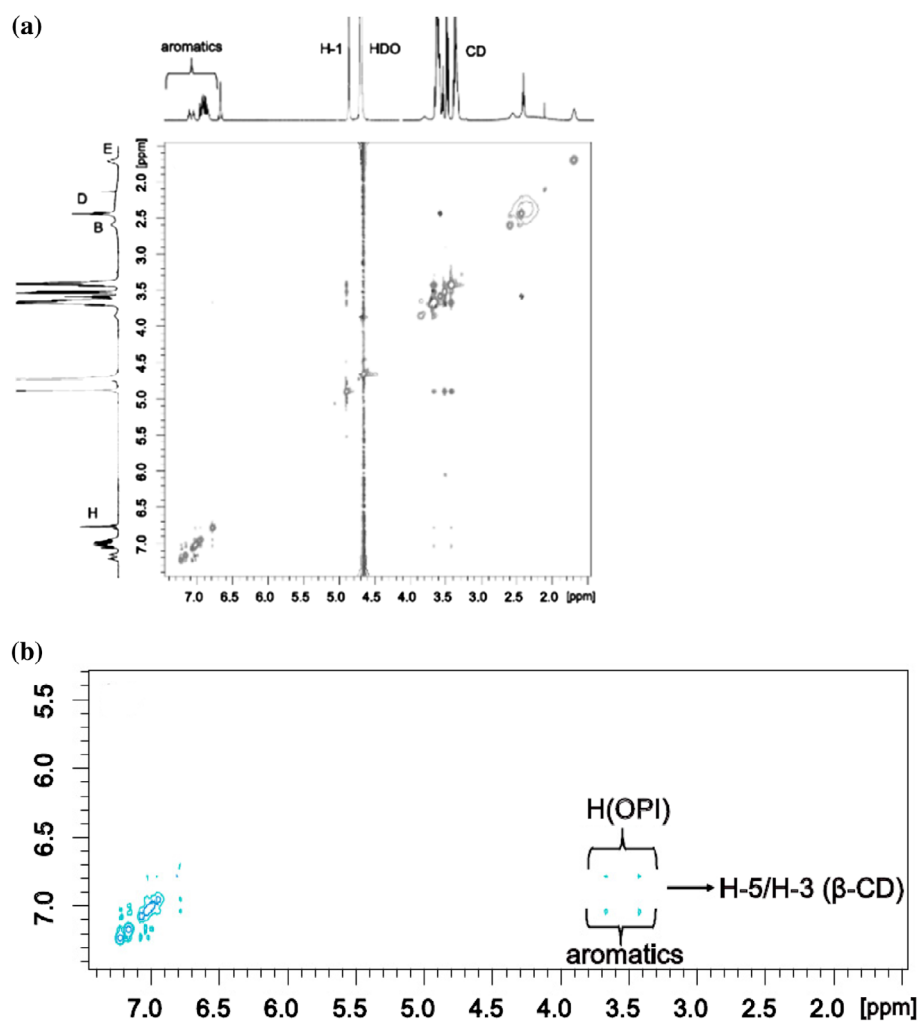


**Figure 8.** (colour online) (a) NOESY spectrum of the OPI- $\beta$ -CD in  $\text{D}_2\text{O}$  at 25 °C; (b) expansion of the NOESY spectrum indicating the aromatic NOE cross peaks between the OPI and  $\beta$ -CD protons.





is only partly incorporated in the cavity of CD and its aliphatic part interacts with the external surface.

The complex spectrum shows many changes in the multiplets appearance. The most spectacular difference occurred for groups named: E (Figure 7 (d) and (e)) and is caused by partial incorporation of only one benzene ring into the cavity of  $\beta$ -CD. As a result, aromatic protons are distinguishable for the groups named: G (Figure 7 (f) and (g)).

A more detailed structure of OPI- $\beta$ -CD complex by proton-proton NOE experiments was obtained. Overhauser effects between the guests molecule and H-3 and H-5 were observed. The 2D NMR spectrum results showed in Figure 8 confirm that the aromatic ring of OPI is included within the CD cavity.

### X-ray diffractometry

The XRD patterns for pure components and their binary systems prepared by two different techniques (CG and FD) at a molar ratio of 1:1 are shown in Figure 9. The creation of an inclusion complex causes significant changes, both in the X-ray diffraction guest and host. The changes were observed in the form of decreased intensity, disappearance, broadening and appearance of new peaks. Due to the crystalline structure of OPI and  $\beta$ -CD in the powder XRD patterns, the sharp and intense peaks were observed. Strong sharp peaks were noticed for OPI at diffraction angles ( $2\theta$ ): 13.81°, 16.11°, 21.49°, 22.39°, and for pure  $\beta$ -CD at diffraction angles ( $2\theta$ ): 9.03°, 12.59°, 17.05°, 22.61°, 27.09°. The diffraction pattern of the investigated PM corresponds to the sum of peaks of those of the pure components. The most intensity peaks were observed at diffraction angles ( $2\theta$ ): 19.43° and 21.25°. Broad peaks were observed in the diffractogram of the inclusion complex, confirming the amorphous nature of the obtained binary systems (29). Thus, by changing the guest molecule from crystalline to the amorphous state, the solubility of OPI may increase (30).

### Scanning electron microscopy

SEM microphotographs of raw material (OPI,  $\beta$ -CD) and prepared binary systems are presented in Figure 10. OPI is characterised by irregular plate structures, whilst  $\beta$ -CD appeared as a parallelogram shape (31). In SEM image of PM, the originals of both components were clearly detectable. OPI existed as irregular crystals separated or adhered to cyclodextrin. Similar results were observed by Gannimani et al. (29) in antipyrine- $\gamma$ -CD and A. Figueiras et al. (32) in the omeprazole- $\beta$ -CD inclusion complex. For systems obtained by the CG and FD methods, visible OPI agglomerated crystals on the surface of  $\beta$ -CD have lost the

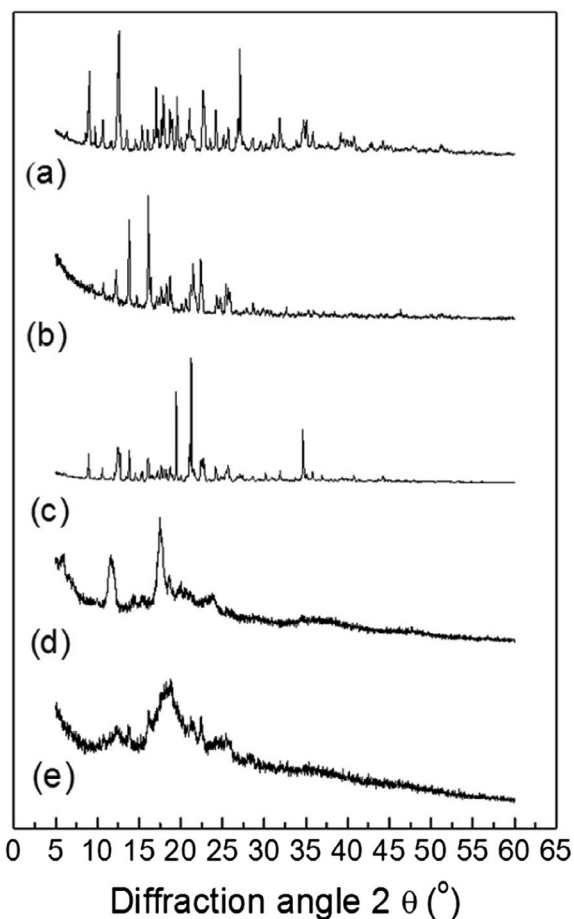


Figure 9. X-ray diffraction patterns of (a)  $\beta$ -CD, (b) OPI, (c) PM, (d) FD and (e) CG inclusion complex.

original shape and were smaller in size. Products appeared to be fluffy and shapeless. These drastic changes in the particle shape in the inclusion complexes confirm interaction between OPI and  $\beta$ -CD leading to the formation of a new solid phase (31, 33).

### Dissolution studies

The release rate is one of the most important features determining an inclusion complex. The dissolution profiles of OPI, OPI (2 HCl) and solid OPI- $\beta$ -CD binary systems are shown in Figure 11. The presented values are the arithmetic mean of three measurements  $\pm$  standard deviations. The per cent amount dissolved active compound for each product was calculated according to the calibration curve for pure OPI. The extent of dissolution after 10, 30 and 60 min ( $DP_{10}$ ,  $DP_{30}$  and  $DP_{60}$ ) is presented in Table 2. Additionally, the dissolution efficiency data calculated based on 60 min ( $DE_{60}$ ) are compiled in Table 3.

For pure opipramol base no complete dissolution was achieved even after 120 min, under the specified dissolution conditions. Due to the hydrophobic properties of the

drug, contact with the dissolution medium was difficult. The slight improvement of OPI extent of dissolution after 60 min obtained when the PM of OPI and  $\beta$ -CD was examined. It can be assigned as a result of two factors. First, is improvement of OPI wettability and/or solubility of the action of the carrier related with local solubilisation, acting in the environment on the hydrodynamic layer surrounding the drug particles. The other key factor is formation 'in-situ' freely soluble complexes in the dissolution medium (34).

A slight increase in the solubility of a PM compared to the pure drug can also be a consequence of mechanical

treatment, because of the drug-CD contact surface was increased (35). After 10 min, the percentage of the dissolved drug is above 15% for the opipramol base, and above 97% when complexed with  $\beta$ -CD.

One-way analysis of variance of  $DE_{60}$  values suggests that there was not a significant difference ( $p > 0.05$ ) between the OPI:  $\beta$ -CD studied systems. For comparison, the dissolution efficiency value of the OPI salt form is similar to the efficiency of the dissolution rate of the formed complexes.

The considerable enhancement of the dissolution efficiency that occurred in the case of received complexes

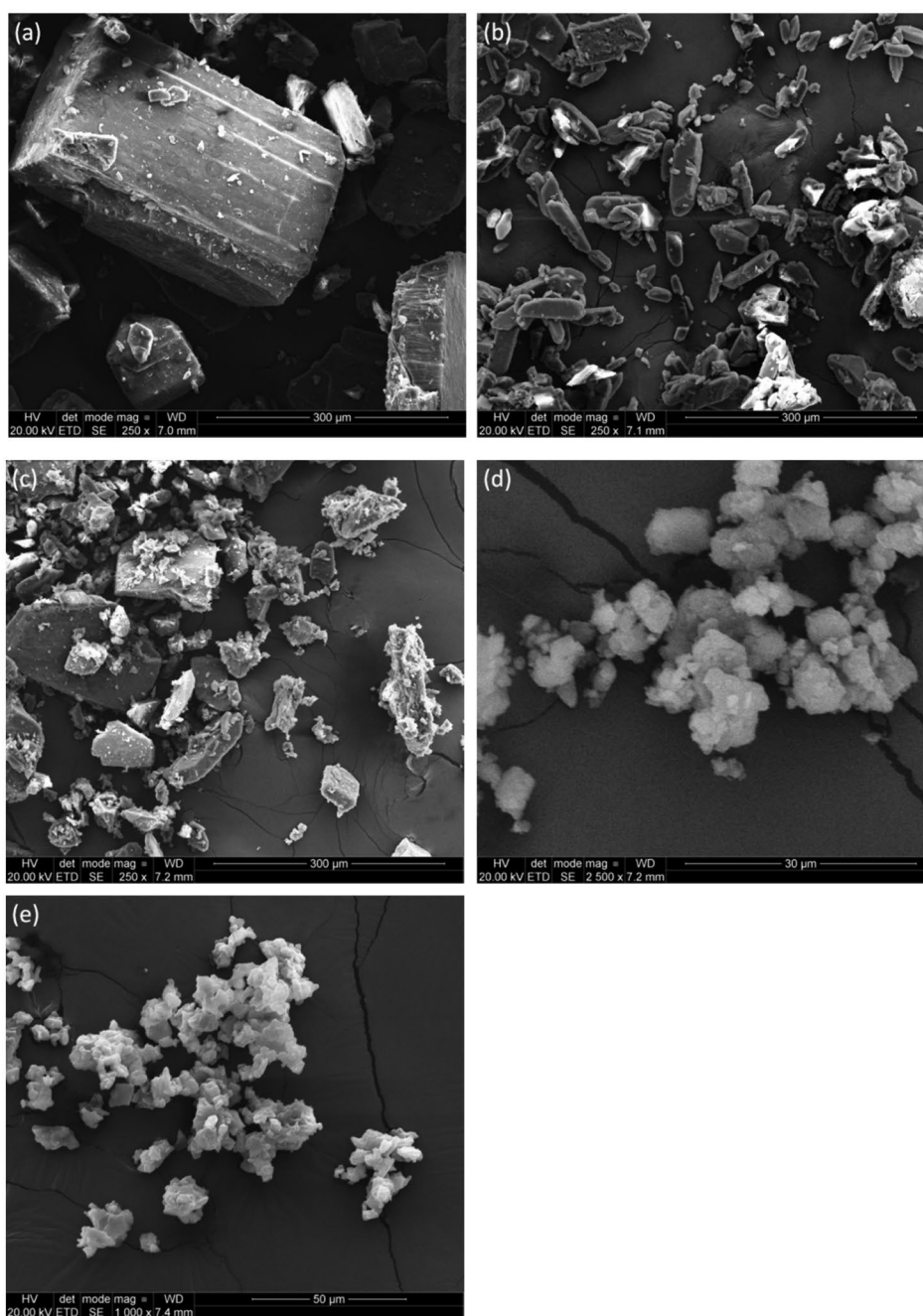
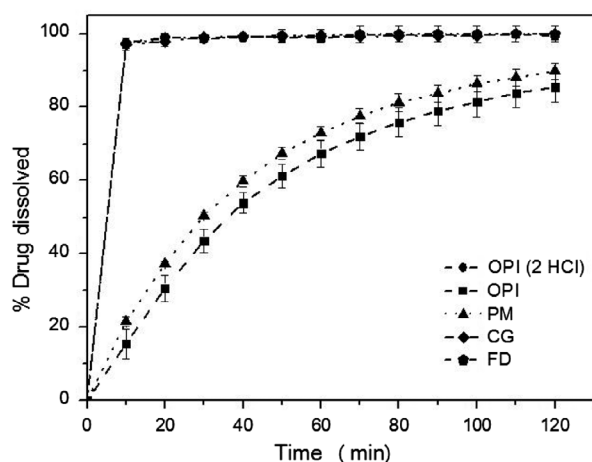


Figure 10. SEM photographs of (a)  $\beta$ -CD, (b) OPI, (c) PM, (d) CG and (e) FD inclusion complex.



**Figure 11.** The dissolution profiles of OPI (2 HCl), OPI and solid OPI- $\beta$ -CD binary systems.

**Table 2.** Dissolution parameters of OPI, OPI (2 HCl), PM, CG and FD binary systems (values are mean  $\pm$  SD,  $n = 3$ ).

System	Extent of dissolution after 10 min (DP <sub>10</sub> %)	Extent of dissolution after 30 min (DP <sub>30</sub> %)	Extent of dissolution after 60 min (DP <sub>60</sub> %)
OPI	15.5 $\pm$ 4.1	43.6 $\pm$ 3.1	67.4 $\pm$ 3.6
OPI (2 HCl)	97.5 $\pm$ 0.5	98.6 $\pm$ 1.0	98.8 $\pm$ 1.2
PM	21.6 $\pm$ 1.3	50.4 $\pm$ 0.8	72.9 $\pm$ 1.9
CG	97.1 $\pm$ 0.9	99.1 $\pm$ 0.4	99.4 $\pm$ 0.6
FD	97.3 $\pm$ 1.7	99.0 $\pm$ 1.0	99.5 $\pm$ 1.6

**Table 3.** DE<sub>60</sub> of OPI, OPI (2 HCl), PM, CG and FD binary systems (values are mean  $\pm$  SD,  $n = 3$ ).

System	Dissolution efficiency (DE <sub>60</sub> %)
OPI	77.9 $\pm$ 7.0
OPI (2 HCl)	99.6 $\pm$ 0.7
PM	82.8 $\pm$ 6.0
CG	99.6 $\pm$ 0.7
FD	99.9 $\pm$ 1.7

with  $\beta$ -CD may be explained: (1) improve of OPI solubility upon complexation in the solid state; (2) amorphous state/ reduction of the crystallinity following complexation (this result is confirmed by XRD studies); (3) surfactant-like properties of cyclodextrin, which can reduce the interfacial tension between the dissolution medium and water-insoluble drugs (34).

From this analysis, we can conclude that the FD and CG techniques were appropriate to achieve complexation, confirmed by physicochemical modification in the solid complexes compared to the PM.

## Conclusions

A novel solid binary system of OPI with  $\beta$ -CD was prepared using CG and FD techniques. The phase-solubility

diagram presents the formation of a 1:1 inclusion complex OPI- $\beta$ -CD. Complex formation was confirmed by DSC, TGA, FTIR, <sup>1</sup>H NMR, XRD and SEM. According to the UV-vis method, the enhancement of OPI solubility in water compared to the pure drug was observed. The dissolution of the opipramol base was enhanced in both systems, and the results were similar to the dissolution results obtained for commercially available opipramol dihydrochloride. Considering the obtained results, it can be assumed that proposed binary systems might improve water solubility of the opipramol base without changing the therapeutic effect and allow for the use of more economical and environmentally friendly method of production of this pharmaceutical.

## Acknowledgements

The authors would also like to thank Ph.D. Ewa Paluszkiwicz, Ph.D. D. Sc. Anna Dołęga, Ph.D. Jakub Karczewski and MSc Maja Szczepańska for contribution to the experimental work. Authors express gratitude to professor Małgorzata Sznitowska and professor Jan Biernat for their valuable scientific discussion.

## Disclosure statement

No potential conflict of interest was reported by the authors.

## Funding

The authors are grateful for financial support provided by the Gdańsk University of Technology [grant number BW 020223/003].

## References

- (1) Savjani, K.T.; Gajjar, A.K.; Savjani, J.K. *ISRN Pharm.* **2012**, *2012*, 1–10.
- (2) Sharma, D.; Soni, M.; Kumar, S.; Gupta, G. *Res. J. Pharm. Technol.* **2009**, *2*, 220–224.
- (3) Szejtli, J. *Trends Biotechnol.* **1989**, *7*, 170–174.
- (4) Stella, V.J.; Rao, V.M.; Zannou, E.; Zia, V.V. *Adv. Drug Deliv. Rev.* **1999**, *36*, 3–16.
- (5) Viernstein, H.; Köhler, G.; Wolschann, P. *J. Incl. Phenom. Macrocycl. Chem.* **1996**, *25*, 129–132.
- (6) Higuchi, T.; Connors, K.A. *Adv. Anal. Chem. Instrum.* **1965**, *4*, 117–212.
- (7) Khan, K.J. *Pharm. Sci. Pharmacol.* **1975**, *27*, 48–49.
- (8) Loftsson, T.; Hreinsdóttir, D.; Másson, M. *Int. J. Pharm.* **2005**, *302*, 18–28.
- (9) Mihajlovic, T.; Kachrimanis, K.; Graovac, A.; Djuric, Z.; Ibric, S. *AAPS Pharm. Sci. Tech.* **2012**, *13*, 623–631.
- (10) Buchanan, C.M.; Buchanan, N.L.; Edgar, K.J.; Ramsey, M.G. *Cellulose.* **2006**, *14*, 35–47.
- (11) Blanko, J.; Vila-Jato, J.L.; Otero, F.; Anguiano, S. *Drug Dev. Ind. Pharm.* **1991**, *17*, 948–957.
- (12) Akbari, B.V.; Valaki, B.P.; Mardiyah, V.H.; Akbari, A.K.; Vidyasagar, G. *Int. J. Pharm. Technol.* **2011**, *3*, 1842–1859.

- (13) Wang, H.Y.; Han, J.; Feng, X.G. *Spectrochimica Acta Part A*. **2007**, *66*, 578–585.
- (14) Li, N.; Zhang, Y.; Wu, Y.; Xiong, X. *J Pharmaceut Biomed*. **2005**, *39*, 824–829.
- (15) Rossel, C.V.P.; Carreño, J.S.; Rodríguez-Baeza, M.; Alderete, J.B. *Quim. Nova*. **2000**, *23*, 749–752.
- (16) Pinto, L.M.A.; Fraceto, L.F.; Santana, M.H.A.; Pertinhez, T.A.; Oyama, S.J.; de Paula, E. *J. Pharm. Biomed. Anal.* **2005**, *39*, 956–963.
- (17) Yap, K.L.; Liu, X.; Thenmozhiyal, J.C.; Ho, P.C. *Eur. J. Pharm. Sci.* **2005**, *25*, 49–56.
- (18) Mura, P.; Bettinetti, G.P.; Cirri, M.; Maestrelli, F.; Sorrenti, M.; Catenacci, L. *Eur. J. Pharm. Biopharm.* **2005**, *59*, 99–106.
- (19) Badr-Eldin, S.M.; Elkheshen, S.A.; Ghorab, M.M. *Eur. J. Pharm. Biopharm.* **2008**, *70*, 819–827.
- (20) Roik, N.; Belyakova, L. *Phys. Chem. Solid State*. **2011**, *1*, 168–173.
- (21) Roeges, N.P.G. *A Guide to the Complete Interpretation of Infrared Spectra of Organic Structures*; Journal of Chemical Education, Wiley: New York, **1995**.
- (22) György, V.; László, L. *Assignments for Vibrational Spectra of Seven Hundred Benzene Derivatives*; Wiley: New York, **1974**.
- (23) Mary, Y.S.; Panicker, C.Y.; Kavitha, C.N.; Yathirajan, H.S.; Siddegowda, M.S.; Cruz, S.M.A.; Nogueira, H.I.S.; Al-Saadi, A.A.; Van Alsenoy, C.; War, J.A. *Spectrochim Acta A Mol Biomol Spectrosc.* **2015**, *137*, 547–559.
- (24) Tang, B.; Chen, Z.-Z.; Zhang, N.; Zhang, J.; Wang, Y. *Talanta*. **2006**, *68*, 575–580.
- (25) Hamdi, H.; Abderrahim, R.; Meganem, F. *Spectrochim Acta A Mol Biomol Spectrosc.* **2010**, *75*, 32–36.
- (26) Dua, K.; Pabreja, K.; Ramana, M.V.; Lather, V.J. *Pharm. Bioallied Sci.* **2011**, *3*, 417–425.
- (27) Ogawa, N.; Hashimoto, T.; Furuishi, T.; Nagase, H.; Endo, T.; Yamamoto, H.; Kawashima, Y.; Ueda, H. *J. Pharm. Biomed. Anal.* **2015**, *107*, 265–272.
- (28) Desai, N.S.; Bramhane, D.M.; Nagarsenker, M.S. *J. Incl. Phenom. Macrocycl. Chem.* **2011**, *70*, 217–225.
- (29) Gannimani, R.; Perumal, A.; Ramesh, M.; Pillay, K.; Soliman, M.E.; Govender, P. *J. Mol. Struct.* **1089**, *2015*, 38–47.
- (30) Periasamy, R.; Rajamohan, R.; Kothainayaki, S.; Sivakumar, K. *J. Mol. Struct.* **1068**, *2014*, 155–163.
- (31) Lee, P.S.; Han, J.Y.; Song, T.W.; Sung, J.H.; Kwon, O.; Song, S.; Chung, Y.B. *Int. J. Pharm.* **2006**, *316*, 29–36.
- (32) Figueiras, A.; Carvalho, R.A.; Ribeiro, L.; Torres-Labandeira, J.J.; Veiga, F.J.B. *Eur. J. Pharm. Biopharm.* **2007**, *67*, 531–539.
- (33) Dandawate, P.; Vemuri, K.; Khan, E.M.; Sritharan, M.; Padhye, S. *Carbohydr. Polym.* **2014**, *108*, 135–144.
- (34) Moyano, J.R.; Gines, J.M.; Arias, M.J.; Rabasco, A.M. *Int. J. Pharm.* **1995**, *114*, 95–102.
- (35) Fernandes, C.M.; Vieira, M.; Veiga, F.J.B. *Eur. J. Pharm. Sci.* **2002**, *15*, 79–88.

